The sulphatic Haselgebirge evaporite mélange of the Moosegg quarry, central Northern Calcareous Alps

A. Schorn, F. Neubauer, M. Bernroider, J. Genser

10TH ANNIVERSARY 15-20|SEPT SALZBURG
PANGEO AUSTRIA 2012

Exkursion 01
2012 - 09 - 15

TABLE OF CONTENTS

FIGURES

TABLES

1. Introduction

For the reconstruction of Alpine tectonics, the Permian to Lower Triassic Haselgebirge Fm. of the Northern Calcareous Alps (NCA) (Austria) plays a key role for: (1) the origin of Haselgebirge bearing nappes, (2) the potentially primary or tectonic inclusion of magmatic and metamorphic rocks revealing tectonic processes not preserved in other units, and (3) debated mode of emplacement, namely gravity-driven or tectonic. With these aims in mind, we studied the sulphatic Haselgebirge exposed to the east of Golling, particularly the gypsum quarry Moosegg and its surroundings located in the central NCA (Figs. 1, 2, 3). Here, we show new observations and most important analytical data, which shed significant new insights on the tectonic evolution of this segment of the NCA. For further details, the reader is referred to Schorn (2010), Schorn and Neubauer (2011) and Schorn et al. (Tectonophysics, revision submitted).

In central NCA, the Tirolic units are widespread and nearly subhorizontal within the so-called Tirolic arc (Tollmann, 1985). The overlying Juvavic units are subdivided into the Lower Juvavic unit with the Haselgebirge Fm. and mainly lenses and blocks of Middle-Upper Triassic pelagic limestone of the Hallstatt facies realm. These units are tectonically overlain by the Upper Juvavic units of the Untersberg and Dachstein nappes, and in the study area, by the Schwarzer Berg klippe (Figs. 2, 3). In the Moosegg area, the Haselgebirge Fm. (lower part of the Juvavic nappe), overlying the Lower Cretaceous Rossfeld Fms., forms a tectonic klippe (Moosegg klippe) preserved in a synform, which is cut along its northern edge by the ENE-trending high-angle normal Grubach fault juxtaposing the Haselgebirge Fm. to the Upper Jurassic Oberalm Fm. (Fig. 2). The Lower and Upper Rossfeld Fms. comprise synorogenic clastic sediments (mainly sandstones and subordinate conglomerates; Faupl and Tollmann, 1978; von Eynatten et al., 1996).

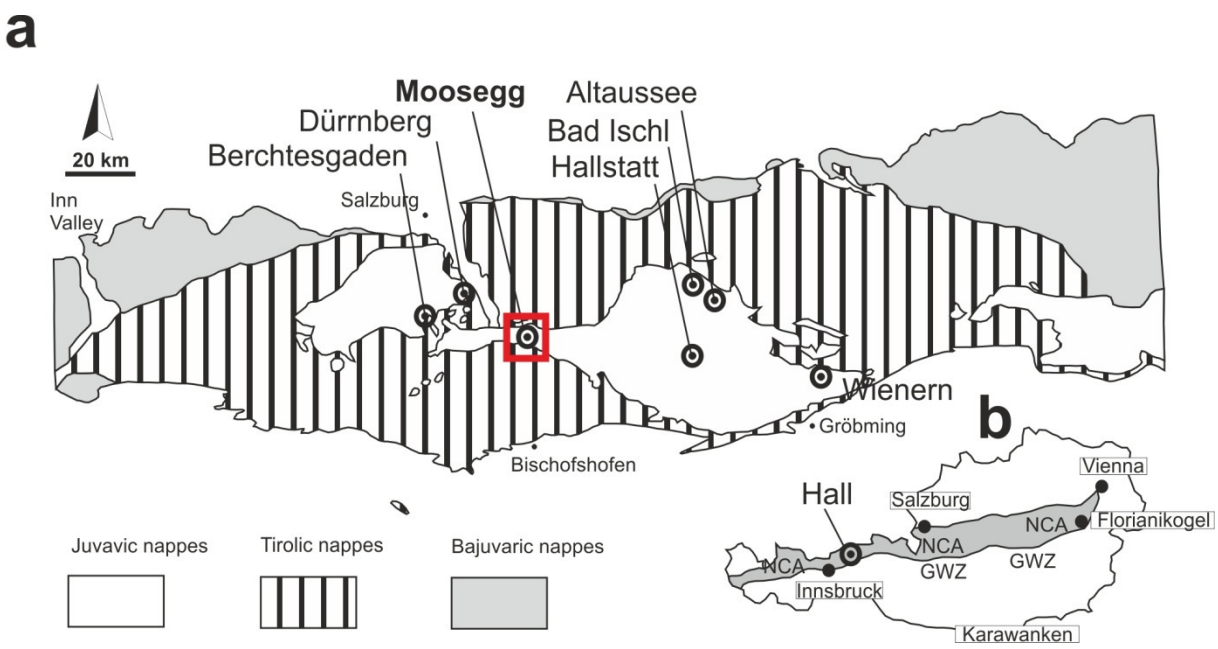

Fig. 1. a - Overview over Austroalpine units in Eastern Alps and Western Carpathians). b - Overview over Austroalpine units in central NCA (modified from Leitner et al., 2011).

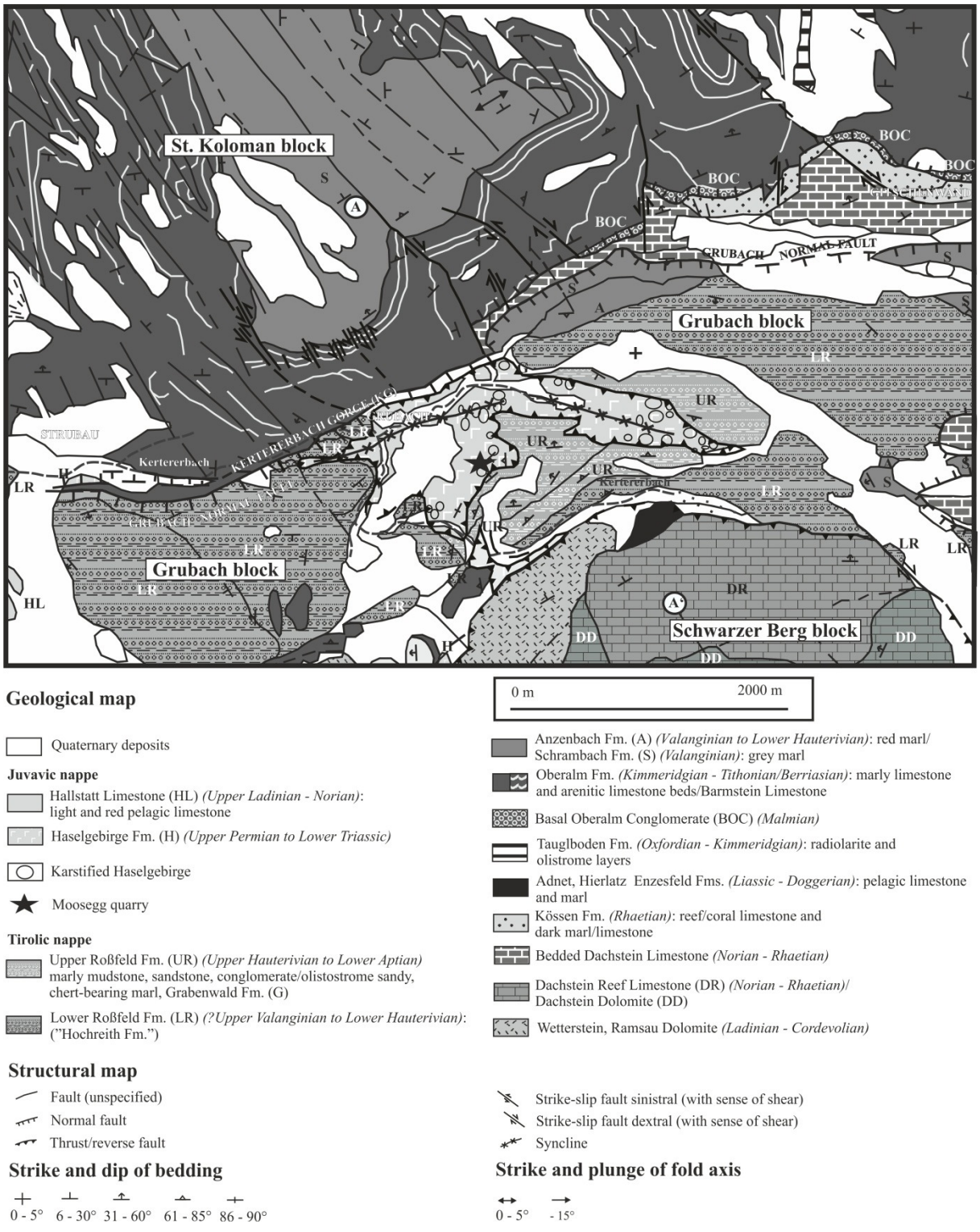

Fig. 2.. Geological map of the central southern part of the Osterhorn Tirolic nappe and overlying units (modified after Geological Map, scale 1:50,000, sheet Hallein (Plöchinger, 1987) updated by own observations); A - A´, section of Figure 3. (modified after Schorn and Neubauer, 2011).

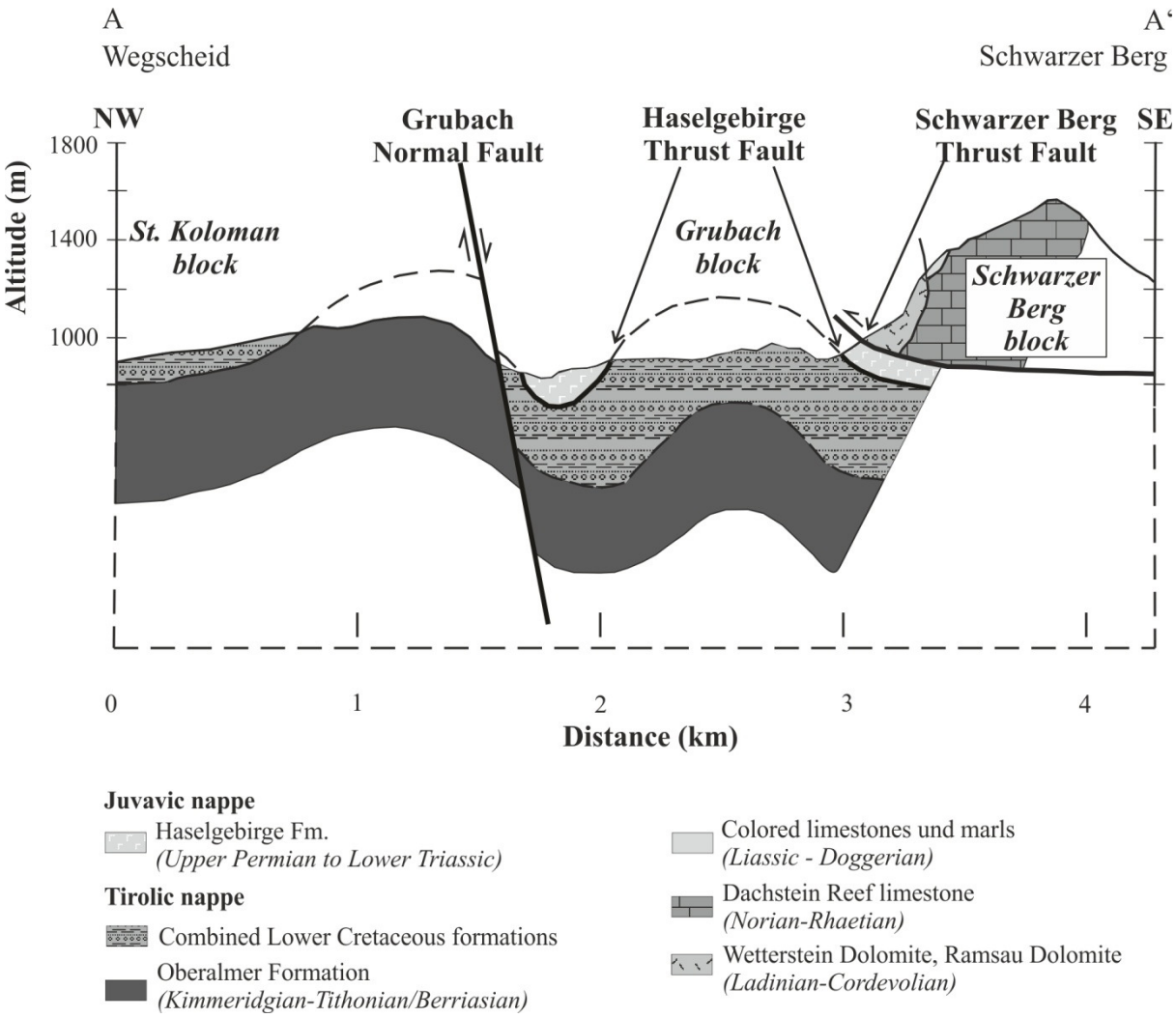

Fig. 3. - Simplified NW-trending section across the study area showing the Moosegg klippe, the Grubach normal fault, the Haselgebirge thrust fault, synclines, anticlines and the Schwarzer Berg thrust fault (after Schorn and Neubauer, 2011).

Fig. 4. Geological map of Moosegg quarry (after Schorn and Neubauer, 2011). The numbers 1 to 9 mark the excursion stops. JN – Juvavic nappe.

2. Lithology and structures of the Moosegg klippe

An overview on the study area and a section is shown in Figures 2 and 3. The gypsum mine Moosegg at Grubach (GPS-coordinates 47°36'56.41 N13°13'00.50 E) (Figs. 4, 5a) was first documented in 1613. Fibrous gypsum of the Moosegg quarry, which was dated by sulphur-isotope measurements, yield an Upper Permian age (Pak, 1978). In the course of our research, the Moosegg quarry was mapped in detail in terms of its geology and geological structure (Figs. 4, 5a). The levels of the quarry were numbered from I to X with increasing altitude.
In principle, the main parts of the quarry are composed of a partly karstified cap of gypsum (Fig. 5a and b). A syncline of light-coloured massive gypsum with lenses of anhydrite in the centre (Petraschek, 1947) (excursion stop 5) is surrounded by more or less foliated dark gypsum breccia. Furthermore, some decimeter- to meter-sized blocks of exotic rocks including different types of plutonic rocks, greenstones and various claystone/mudstones as well as dolomite lenses are of great importance. Furthermore, a carbonatic breccia with red and green claystone and mudstone (Fig. 5f), dark jointed anhydrite (Fig. 5g) and dark gypsum shear bands (Fig. 5j) are observed.
A breccia with a groundmass of gypsum (Fig. 5a and c) makes up the bulk of the quarry, and components vary in size between 1 cm and 1 m. Apart from gypsum and anhydrite clasts they consist of several different types of magmatic rocks. These include biotite-diorite (Figs. 5d, 8a; excursion stop 6), meta-syenite, then meta-doleritic blueschists, ultramafitites, and heavily altered, carbonatic volcanic rocks and a rare, banded meta-psammitic schist (Fig. 8d).
In the south-eastern part of level I (Fig. 6a) ductile structures related to thrusting of the Haselgebirge Fm. over the Lower to lowermost Upper Cretaceous rocks is preserved close to the structural base of the Moosegg klippe in folded, nearly vertically dipping anhydrite and carbonate mylonites (Fig. 6b and d). The carbonate mylonite comprises millimeter-sized pyrite grains with pressure fringes indicating a well-expressed subhorizontal stretching lineation. The banded mylonites are nearly subvertically or steeply N-dipping and folded (Fig. 6c and d). Shear sense criteria indicate a top-west movement of the Haselgebirge nappe (Fig. 7a-d). The banded mylonites are folded with subhorizontal fold axes, here assigned as fold axes F_2, and a cogenetic fracture cleavage S_2 (Fig. 6e).
The Moosegg quarry and its vicinity received a significant thermal overprint reaching a maximum temperature of ca. 290 - 300°C (Table 1).

Table 1. Temperature conditions of eo-Alpine metamorphism within the Moosegg area, central NCA (from Leitner et al., 2011). For full sources, see cited manuscript. CAI - conodont color alteration index, FI - fluid inclusions, VR - vitrinite reflectance.

Location	Method	Temperature range (°C)	Temperature, best estimate (°C)	Author(s)
Northern Calcareous Alps, southern margin	FI	270 - 360	315	Götzinger and Grum (1992)
Sazkammergut, Juvavic nappes	CAI	80 - > 350	80	Gawlick et al. (1994)
Moosegg	FI	220 - 262	240	Spötl et al. (1998)
Moosegg	FI	> 300	300	Wiesheu (1997)
Moosegg	FI	300	300	Wiesheu (1997)
Lammer unit (Juvavic unit)	VR	max. 290	290	Rantitsch and Russegger (2005)

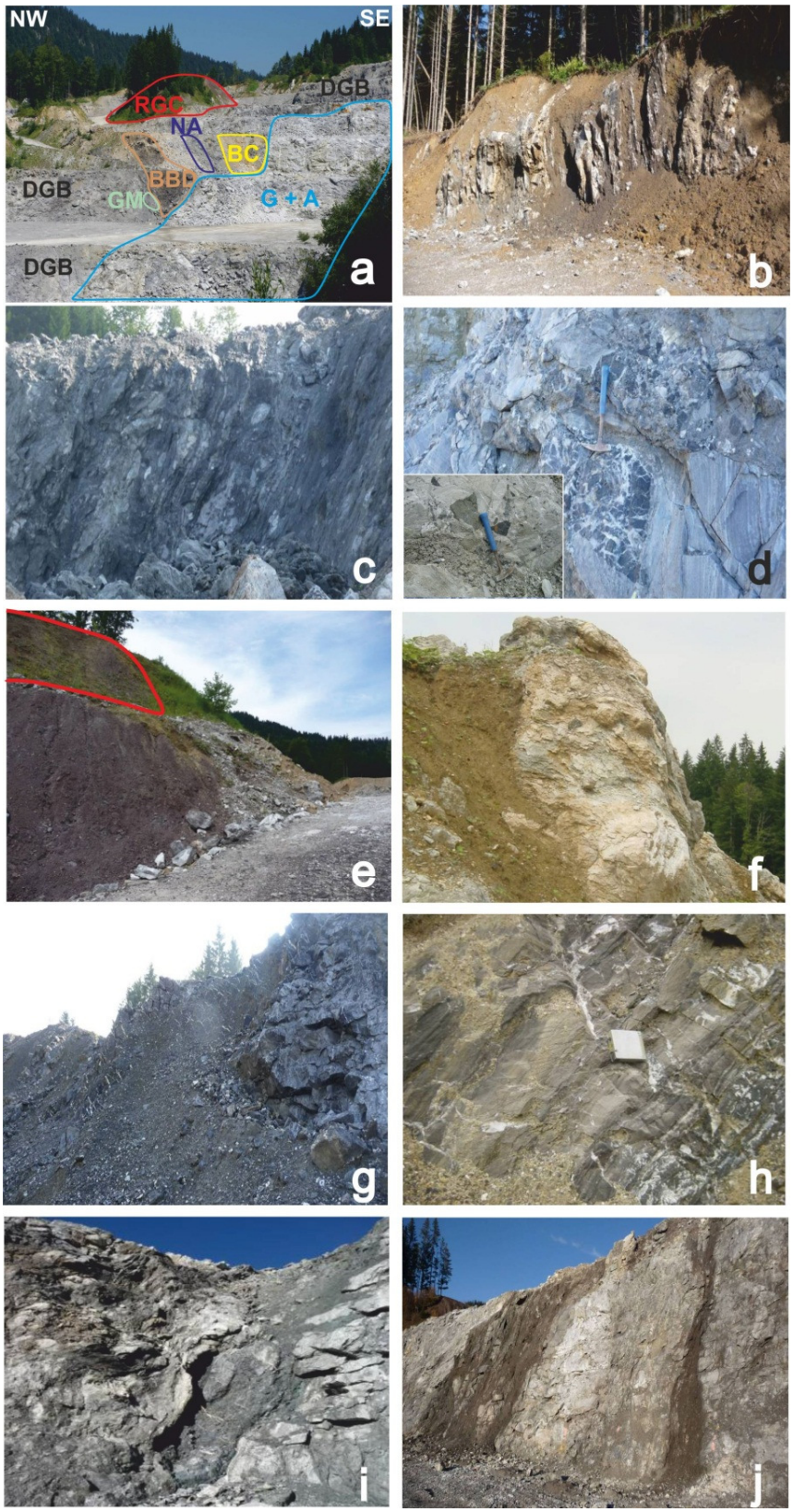

Fig. 5. Field photographs from the lithologies in the Moosegg quarry (after Schorn and Neubauer, 2011). a - Overview of Moosegg quarry: Note the lenses of brown, banded dolomite (BBD), green and dark clayey mudstone (GM), light-brownish claystone (BC), dark anhydrite with fibrous blue Na-amphibole (NA) and red and green claystone (RGC) on the left side and light-coloured white gypsum (G) with small lenses of anhydrite (A) on the right side, embedded in dark, foliated gypsum breccia (DGB). b - Karst caveats in the uppermost part of the quarry. c - Strongly foliated gypsum breccia of level VIII. d - Dark gypsum breccia with two types of dark components of level III containing a well preserved biotite-diorite block (small picture). e - Boundary between grey siliceous marl and rauhwacke (cellular limestone; upper side) and red and green claystone and mudstone. f - Carbonatic breccia with red and green claystone and mudstone. g - Dark jointed anhydrite. h - Brown banded dolomite of level III. i - Dark anhydrite with fibrous blue amphibole. j - Shear zones of level V.

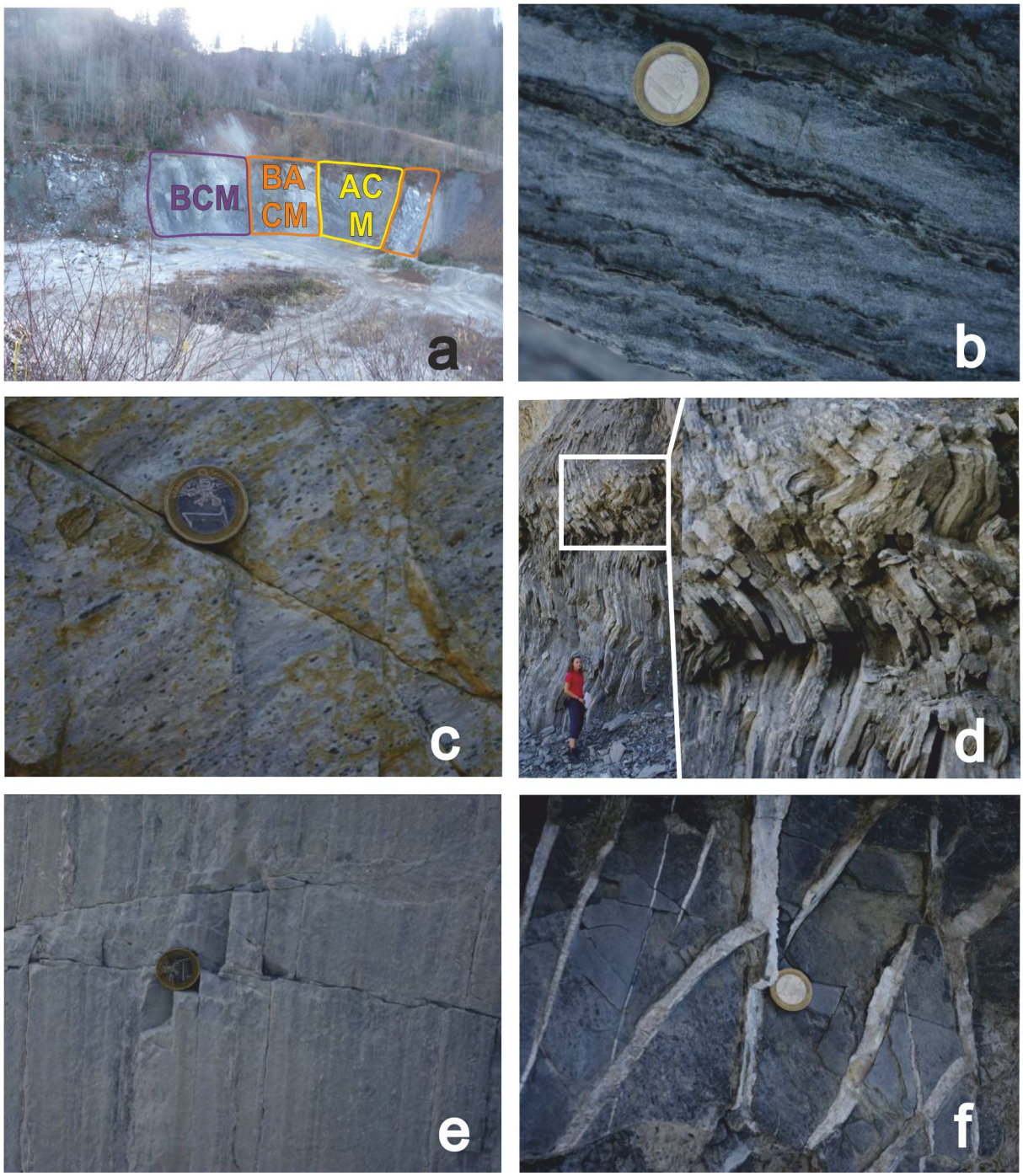

Fig. 6. a - Overview of the southern part of level I with BCM - banded carbonate mylonite, BACM - banded anhydrite-carbonate mylonite and ACM – anhydrite-carbonate mylonite (after Schorn and Neubauer, 2011). b - Foliation in banded anhydrite-carbonate mylonite. The foliation S1 intersects bedding with an acute angle. c - Stretching lineation in banded anhydrite-carbonate mylonite. The stretching lineation is underlined by elongated rigid pyrite porphyroclasts with pressure fringes subparallel to the stretching lineation. d - Well foliated carbonate and anhydrite mylonite with folds at level I of the Moosegg quarry. e - A peculiar case of the fracture cleavage S2 in well foliated carbonate mylonite. f - Gypsum-filled extensional veins. Note two sets of veins and a similar orientation of fibres in both sets. For explanation, see text.

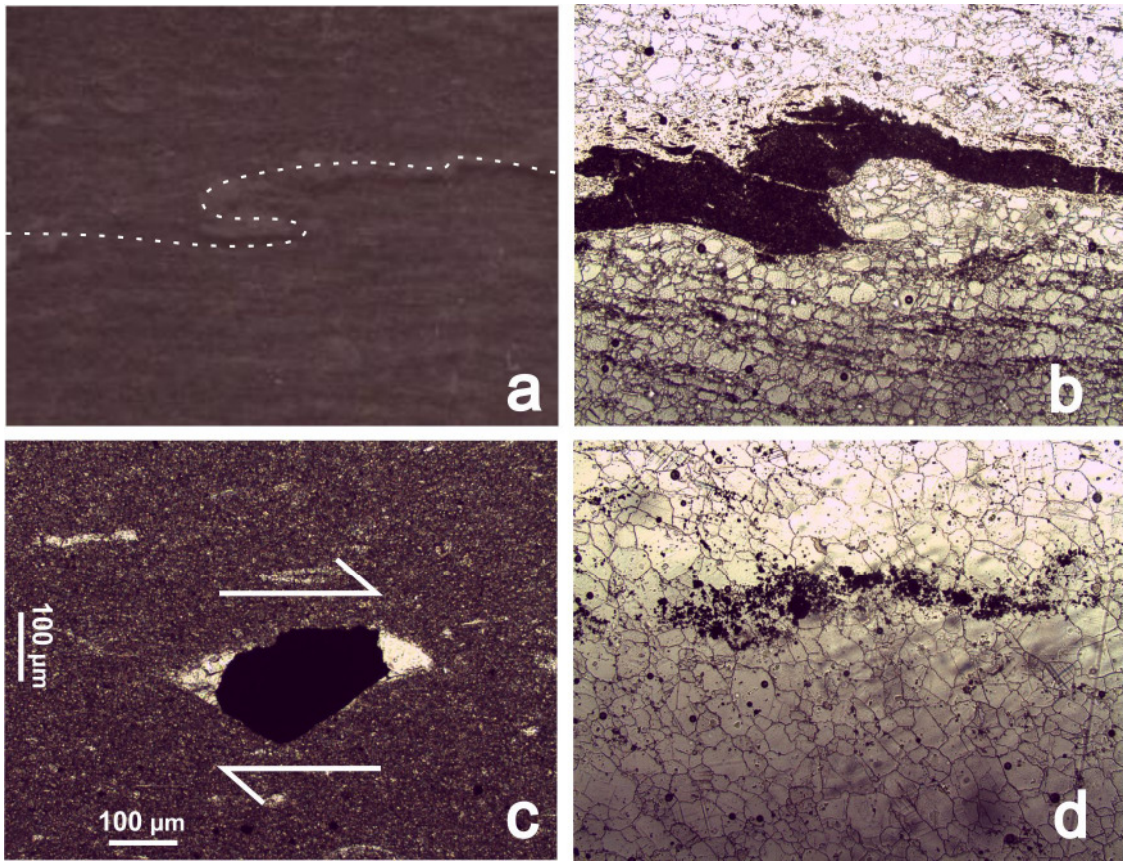

Fig. 7. Examples of shear sense criteria showing top W motion (after Schorn and Neubauer, 2011). a – Thin section-scale isoclinal intrafolial fold (scan of a thin section). b – Microphotograph showing an isoclinal intrafolial fold. c - Asymmetric pressure fringes indication a top west movement. d - Microphotograph showing oblique orientation of subparallel anhydrite grains in respect to elongated subhorizontal aggregates of ore grains.

3. Petrography of magmatic blocks

In the following, a representative sample from each group of rocks is described, which was also used for geochemical investigations. The main emphasis is on preservation of relictic magmatic minerals, the degree and nature of secondary alteration of primary magmatic rocks, and the metamorphic neocrystallization.

The **biotite-diorites** (Figs. 5d, 8a) comprise mostly brown-coloured biotite, which has marginally transformed to leucoxene or a fine-grained aggregate of chlorite and white mica. The more common secondary peripheral change to green biotite is important for the age interpretation. The xenomorphic or lath-shape ore grains (0.1 – 0.5 mm) are often overgrown by brown biotite. Furthermore, the rock contains titanium-rich brown amphibole (kaersutite), which is well preserved in relicts, primarily intergrown with biotite, marginally intergrown with other minerals and fragmented. Some margins are transformed to a fine-grained aggregate (with grains sizes of 0.02 mm) of chlorite, white mica and possibly epidote. Fragments of colourless to pale green actinolite occur, which are also in part frayed marginally. Larger aggregates of plagioclase – presumably oligoclase (15 – 20% anorthite) – are sometimes nearly completely transformed to sericite. Nevertheless, they partly still show polysynthetic twinning. Moreover, pseudomorphs composed of chlorite, secondary green biotite, green actinolite and much clinozoisite and epidote (slightly Ca- and Fe-enriched in the cores) are quite common. The average grain sizes of these minerals vary between 0.05 – 0.1 mm. The thin section also comprises relicts of primary pyroxene, which have transformed to chlorite and actinolite. In addition, there are also abundant leucoxene and apatite grains. The latter are mostly idiomorphic and hexangular but also occur in unusual prolate shapes or as inclusions in plagioclase.

The fabric of the meta-syenite is principally consistent with the other meta-dolerites. Furthermore, it contains, apart from abundant brown biotite, up to 0.2 mm long brown amphibole (kaersutite) with rims of greenish amphibole and some K-feldspar.

The meta-dolerites are a quite fine-grained amphibole-rich rock type, which contain abundant 0.1 to 0.3 mm large brown amphibole (kaersutite) showing a greenish rim, many Ti-mineral inclusions and a partial overgrowth by fine-grained white mica. The thin section also comprises brown biotite with many ore segregations. It is transformed peripherally to green biotite, which is in turn altered marginally to white mica. Furthermore, some rutile grains, large aggregates of epidote and relicts of plagioclase and pyroxene are found. Very fine-grained aggregates are composed of a mixture of fine-grained ore minerals, chlorite, leucoxene and white mica.

The meta-doleritic blueschists comprise a strongly altered bluish amphibole with a doleritic, subvolcanic fabric, which is characterised by intergrown 0.3 – 0.7 mm long and 0.5 mm wide laths of plagioclase and pseudomorphs

after plagioclase. They have mainly been altered to fine-grained sericite with average grain sizes from 0.01 – 0.02 mm, and maximum length of 0.1 mm and carbonate (Fig. 8c). Pseudomorphs of other minerals are less frequent and can be classified into two different types: (1) Dark pseudomorphs are completely decomposed and consist of leucoxene with boundaries diffusely intergrown ore grains and fine-grained relicts of pyroxene (probably orthopyroxene). (2) The second type is characterised by relicts of actinolitic amphibole, epidote and clinopyroxene. Furthermore, the rock partly contains well preserved green amphibole and brown biotite, both minerals sometimes transformed to green biotite, isometric ore grains (probably titanium-magnetite), apatite and secondary chlorite.
The ultramafitite comprises relicts of olivine, which is predominantly serpentinized. Furthermore, relicts of well preserved clinopyroxene showing cleavage and twinning and few box-shaped orthopyroxene grains also occur.
The Banded meta-psammitic schist represents one of the few foliated metamorphic clasts and was found within the brown, banded dolomite. The sample is essential for the (white mica) dating of a metamorphic event in the source rocks of the block embedded within the gypsum breccia and shows a highly ductile metamorphic fabric including foliation and exemplarily well developed isoclinal folding. There are three different types of layers: (1) The light-colored layers represent a quartz-muscovite-biotite schist (Fig. 8d) and are composed of slightly stretched, 0.05 – 0.10 mm long quartz grains with amoeboid grain boundaries and much chlorite. Furthermore, white mica with grain sizes from 0.1 to 0.3 mm occurs, then brown biotite, which is very often intergrown with chlorite, 0.02 mm long ore grains and rare chloritoid. (2) The dark layers are polymineralic and rich in amphibole, strongly corroded, and largely transformed to other minerals. Some relicts of colorless to light green amphibole are zoned. The green/brown amphibole (kaersutite) is overgrown by secondary, blue Na-amphibole (riebeckite) (Fig. 8b). (3) The carbonatic layers are intergrown with chlorite. They contain approximately 10 – 15 modal % of chlorite with ore inclusions indicating an origin from biotite and some white mica. The protolith is probably a quartz-rich sandstone with carbonatic layers.

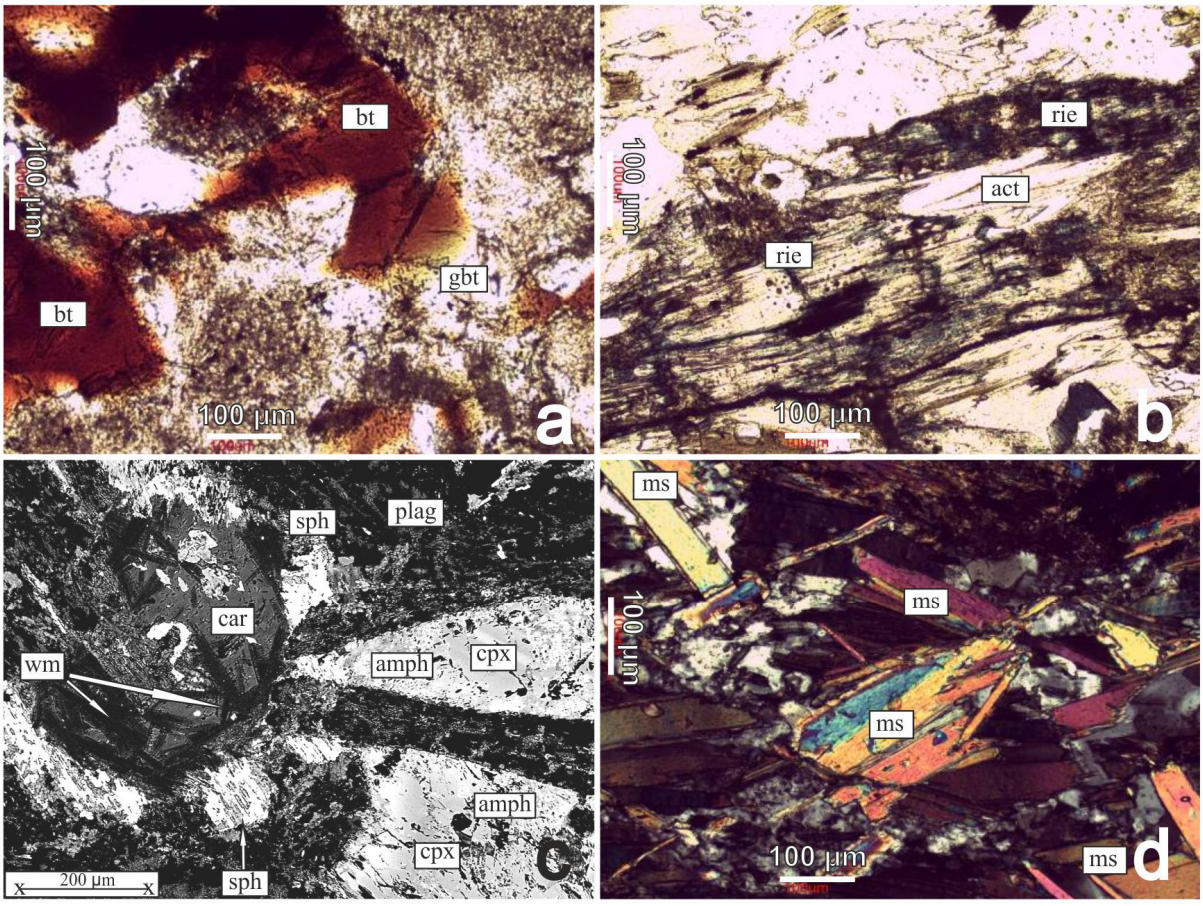

Fig. 8. Photomicrographs (after Schorn et al., Tectonophysics, revision submitted): a - Brown biotite (bt) with peripheral transformation to green biotite (gbt) of thin section IV-E (biotite-diorite), parallel polarizers. b - Amphibole (actinolithe – act), overgrown by secondary, blue Na-amphibole (riebeckite - rie) of II-A (banded meta-psammitic schist), parallel polarizers. c - Back-scattered electron image showing fabrics the meta-doleritic blueschist III-T with relictic cpx-cores with blue amphibole rims (winchite-ferro winchite), strong exsolution phenomena in magmatic minerals and celadonite-rich white mica and carbonate pseudomorphs after plagioclase. Sample III-T. Abbreviations: amph – amphibole, car – carbonate, cpx – clinopyroxene, plag – plagioclase, sph – sphene, wm – white mica. d - Quartz-muscovite-biotite schist layer of II-A (banded meta-psammitic schist) ms - muscovite, crossed polarizers.

4. Composition of magmatic minerals in biotite-diorite

We selected a few samples with well preserved magmatic minerals from the biotite-diorite, meta-dolerite, meta-syenite and meta-doleritic blueschist for microprobe work. We investigated various minerals of the biotite-diorite and here only report data from the kaersutitic amphiboles and their rims and from clinopyroxene, which are important for the interpretation of the tectonic setting of the magmatic suite. Representative analytical results are graphically shown in Fig. 9.
Clinopyroxene occurs in the core of partly well preserved grains or in shape relicts, which are surrounded by a fine-grained mixture of blue amphibole rims (winchite – ferro-winchite). Celadonite-rich white mica and carbonate pseudomorphs after plagioclase are abundant. In the same rock type, brownish kaersutitic amphibole is observed (Fig. 8c). Clinopyroxene is mostly augite (Fig. 9a). The brownish amphibole is kaersutite and the rims are composed of actinolite (Fig. 9b and c).

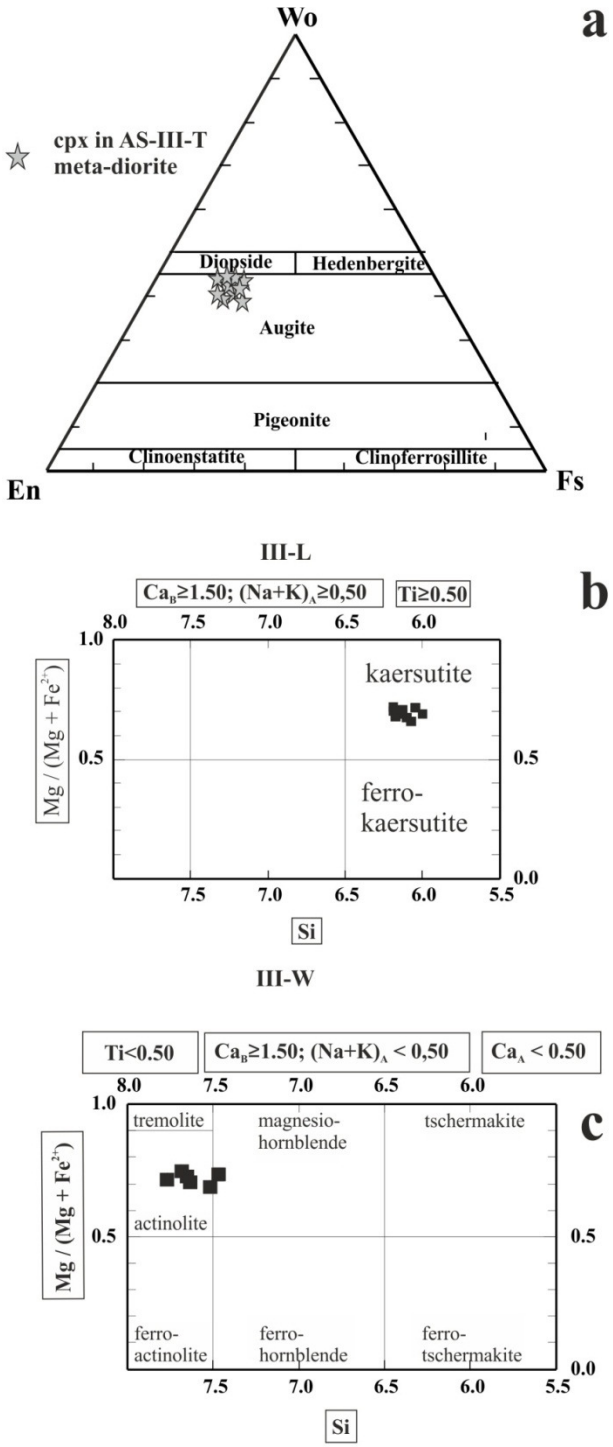

Fig. 9. Composition of a - Clinopyroxene, b - Kaersutitic amphibole and c - Actinolite of biotite-diorite and meta-dolerite (after Schorn et al., Tectonophysics, revision submitted).

5. Geochemistry of magmatic blocks

We used the TAS (total alkalies-silica) graph for plutonics after Cox et al. (1979) (Fig. 10a). One of the meta-dolerites plots near the ijolite field, the remaining others plot close to the gabbro field just as the biotite diorites and one of the meta-dolerites. The meta-dolerites are located near the meta-syenite within the nepheline-syenite field. We also used the Q'(F')-ANOR discrimination diagram for plutonics of Streckeisen and LeMaitre (1979; not shown). The meta-dolerites are located in the fields of foid-syenite, foid -monzonite, foid-monzodiorite and foid-monzogabbro. The biotite-diorite samples plot in the foid-monzodiorite and foid-monzogabbro fields. The meta-dolerites show a broad distribution: they plot in the monzo-gabbro/diorite field as well as on the border of foid-syenite to foid-monzonite and together with the meta-syenites in the foid-syenite fields.
In the following multi-variation diagram analysis, we distinguish five different rock types. The REE (normalized CI chondrite after McDonough and Sun, 1995) (Fig. 10c) of meta-dolerite and meta-syenite are extremely enriched (thousand-fold) with light rare earth elements, which is typical for alkaline magmatites (e.g., from rifts). Furthermore, they show a high La/Lu ratio and a characteristic negative Eu anomaly, which is caused by a plagioclase fractionation in the melt. The meta-doleritic blueschist shows a plain pattern with low enrichment in elements and no Eu-anomaly, which means that plagioclase has never been removed from the melt. The La concentration is lower than that of Ce, which is particular for N-MORB (normal mid-ocean ridge basalt) or T-MORB (transitional MORB) rocks. Together, these samples are very meaningful and surely indicate an N-MORB-origin of blue meta-dolerites. The biotite-diorite samples show a significant enrichment in REEs but no negative Eu-anomaly. Both facts are representative for alkaline rocks. In the Ta/Yb–Th/Yb discrimination diagram after Pearce (1982) (Fig. 10b), the meta-doleritic blueschist plots in the MORB field, the biotite-diorites and one meta-dolerite in the alkaline transition zone. The remaining meta-dolerites are assigned to the shoshonite–calkalkaline field and the meta-syenite to the volcanic arc basalts.
The ultramafitite sample shows a flat pattern and is notably less enriched in all elements than the previous rocks. It also has no Eu-anomaly, which is typical for ultramafic rocks. This rock represents a cumulate, which probably developed from the parent melt of the meta-doleritic blueschist protolith.
In the multi-variation diagram of trace elements versus primitive mantle composition using normalization values of Sun and McDonough (1989), all samples show more or less flat patterns with partially very distinct anomalies (Fig. 10d). They are all enriched with Cs and Rb and show, except for the blue meta-dolerite samples, a prominent negative Ba anomaly.
We suggest that both the blue meta-dolerites and biotite-diorites derived from a primitive mantle melt. The meta-doleritic blueschists show an affinity to MOR basalts while the biotite-diorites originate from the alkaline milieu of a shallow magma chamber without any influence of a subduction zone. In detail, the results are as follows. The meta-dolerites and the meta-syenite show positive anomalies of Cs, Rb, Th, La/Ce, Pr, Nd, Sm, Y and a negative one for Nb, Ta and Ba. The metadoleritic blueschist bears positive anomalies in Cs, Rb and Pb as well as a slightly negative one in Ba. Biotite-diorites exhibit positive anomalies for Cs, Rb, Pb and Sr. The ultramafitite shows positive anomalies for U, Pb, Sr and negative ones for Nb, Sm and Hf.

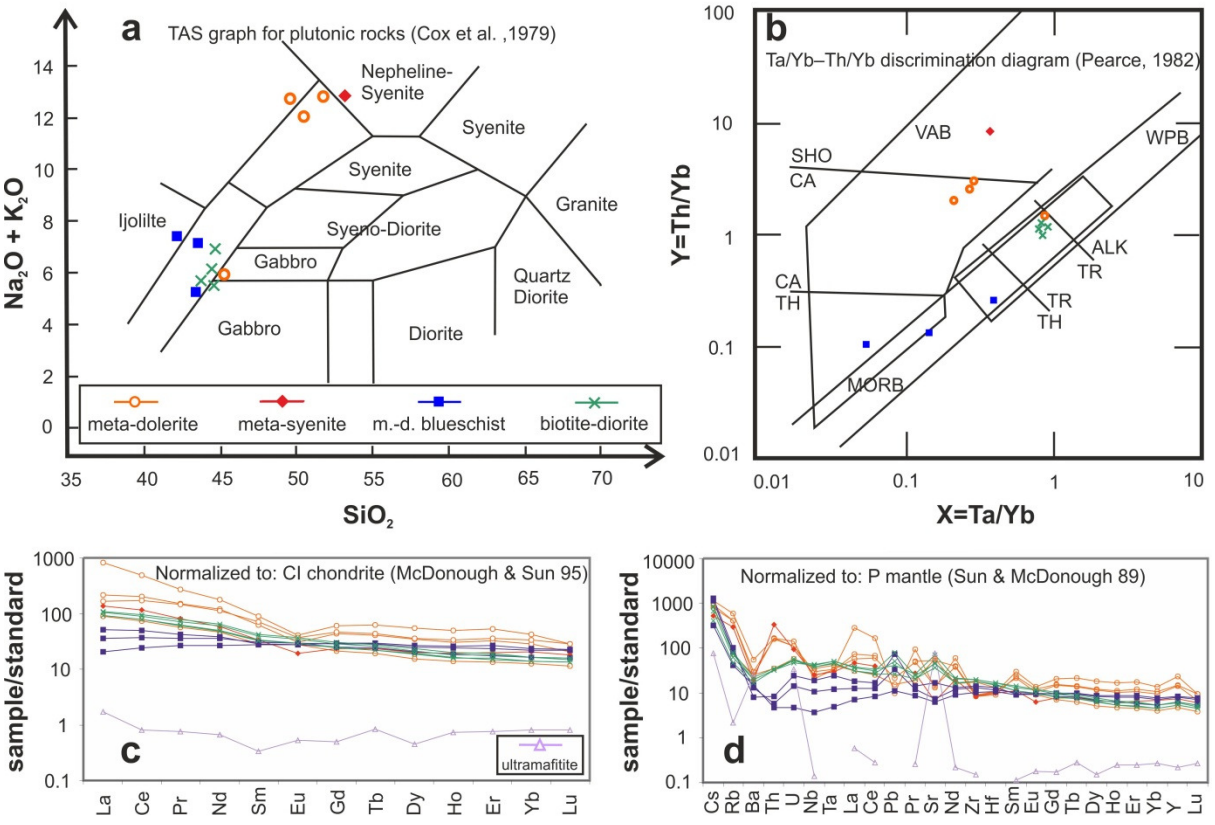

Fig. 10. a -TAS (Total Alkalies-Silica) graph for plutonic rocks according to Cox et al. (1979). b - Ta/Yb–Th/Yb discrimination diagram according to Pearce (1982). VAB - volcanic arc basalt, SHO - shoshonite, CA - calcalkaline, TH - tholeiitic, MORB - mid ocean ridge basalt, TR - trachytic , ALK - alkaline, WPB - within plate basalt. c - Spider diagram normalized to CI chondrite (McDonough and Sun, 1995). d - Multi-element variation diagram All Trace P mantle (Sun and McDonough, 1989); m.-d. blueschist – meta-doleritic blueschist (after Schorn et al., Tectonophysics, revision submitted).

6. Age dating results on magmatic and metamorphic minerals

As mentioned above within the Moosegg quarry of central NCA gypsum/anhydrite bodies are tectonically mixed with lenses of sedimentary rocks and decimeter- to meter-sized tectonic clasts of plutonic and subvolcanic rocks and rare metamorphics. We examined various types of (1) widespread biotite-diorite, meta-syenite (2) meta-dolerite and rare ultramafic rocks (serpentinite, pyroxenite) as well as (3) rare metamorphic banded meta-psammitic schists and meta-doleritic blueschists. For the first time, plutonic and subvolcanic rocks and rare metamorphics were found in the Upper Permian to Lower Triassic Haselgebirge Fm.

The $^{40}Ar/^{39}Ar$ biotite ages from three biotite-diorite, meta-dolerite and meta-doleritic blueschist samples with variable composition and fabrics range from 248 to 270 Ma (e.g., 251.2 ± 1.1 Ma) (Fig. 11) indicating a Permian age of cooling after magma crystallization or metamorphism. The chemical composition of biotite-diorite and meta-syenite indicates an alkaline trend interpreted to represent a rift-related magmatic suite. These and Permian to Jurassic sedimentary rocks were incorporated during Cretaceous nappe emplacement forming the sulphatic Haselgebirge mélange. The scattered $^{40}Ar/^{39}Ar$ white mica ages of a meta-doleritic blueschist (of N-MORB origin) and banded meta-psammitic schist are at ca. 349 and 378 Ma (Fig. 11), respectively, proving the Variscan age of pressure-dominated metamorphism. These ages are similar to detrital white mica ages reported from the underlying Rossfeld Fms., indicating a close source-sink relationship. According to our new data, the Haselgebirge bearing nappe was transported over the Lower Cretaceous Rossfeld Fms., which include many clasts derived from the Haselgebirge Fm. and its exotic blocks deposited in front of the incoming nappe comprising the Haselgebirge Fm. (Fig. 12b).

(U-Th-Sm)/He apatite ages of two biotite-diorite samples (IV-E and IV-F) show two different age groups at ~ 25-27 Ma and ~ 12 Ma. These ages were measured at the (U-Th-Sm)/He Laboratory at Göttingen (István Dunkl). We consider the younger as the significant one. This might indicate that a cooling below 60°C has taken place after 12 Ma and that the sedimentary cover, which was about 2 km thick, was eroded after 12 Ma.

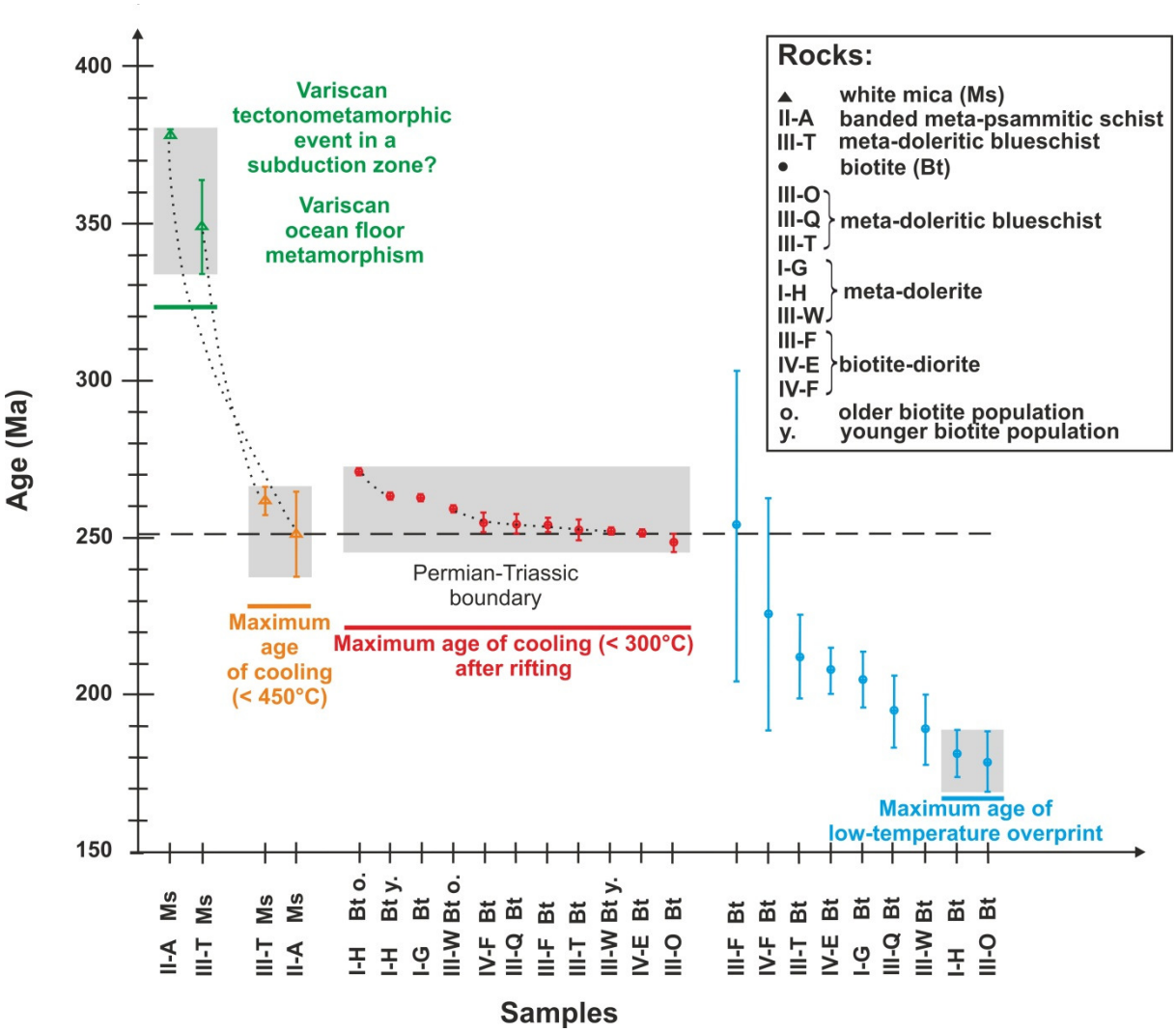

Fig. 11. Diagram showing the 40Ar/39Ar ages of all samples and their interpretation. For explanation, see text (after Schorn et al., Tectonophysics, revision submitted).

7. Tectonic models

At the base of the Haselgebirge Fm., strongly foliated fine-grained anhydrite-carbonate mylonite is preserved with a WNW-trending stretching lineation together constituting a L-S fabric indicating emplacement of the Haselgebirge evaporite mélange within ductile conditions. In other places at the base of the Haselgebirge, anhydrite is transformed into foliated gypsum leaving behind a still well preserved L-S fabric. The main Haselgebirge body comprises foliated, massive and brecciated anhydrite and gypsum. Gypsum breccias with foliated gypsum clasts are quite common, and some of these breccia lenses are again foliated and clasts are stretched implying several stages of ductile deformation. Because of peculiar fabrics, we interpret formation of gypsum and anhydrite breccia by fluid overpressure, possibly in part related to dehydration reactions of gypsum to anhydrite.

For Late Permian, we propose an asymmetric rift setting (Fig. 12a) with a principally ductile low-angle normal fault cutting through the whole lithosphere. This causes the following consequences, which fit with all the observations. The initial rift resulted in the formation of a halfgraben which is filled by clastic sediments exposed along the southern margin of the NCA. We interpret this stage as the synrift phase. In an advanced stage of rifting, mantle melts were produced through an uprise of an asthenospheric dome, which is shifted towards the upper plate. A few gabbroic bodies intruded into a high level of the crust and a few volcanic successions are known, specifically from the eastern Salzkammergut area (e. g., Grundlsee; Kirchner, 1979; Vózarova et al., 1999). These volcanic rocks are in direct contact with Haselgebirge which argues for an emplacement during deposition of the evaporites. We interpret the time of deposition of the Haselgebirge as post-rift phase.

The new (U-Th-Sm)/He apatite ages of ~ 12 Ma indicate a Miocene denudation of ca. 2 km thick sedimentary coverburden (“Augenstein” Fm.) from the Oligocene Dachstein plateau. This is significantly younger as suggested before (Frisch et al., 2001).

As mentioned above the Haselgebirge bearing nappe was transported over the Lower Cretaceous Rossfeld Fms., which include many clasts derived from the Haselgebirge Fm. and its exotic blocks deposited in front of the incoming nappe comprising the Haselgebirge Fm. (Fig. 12b).

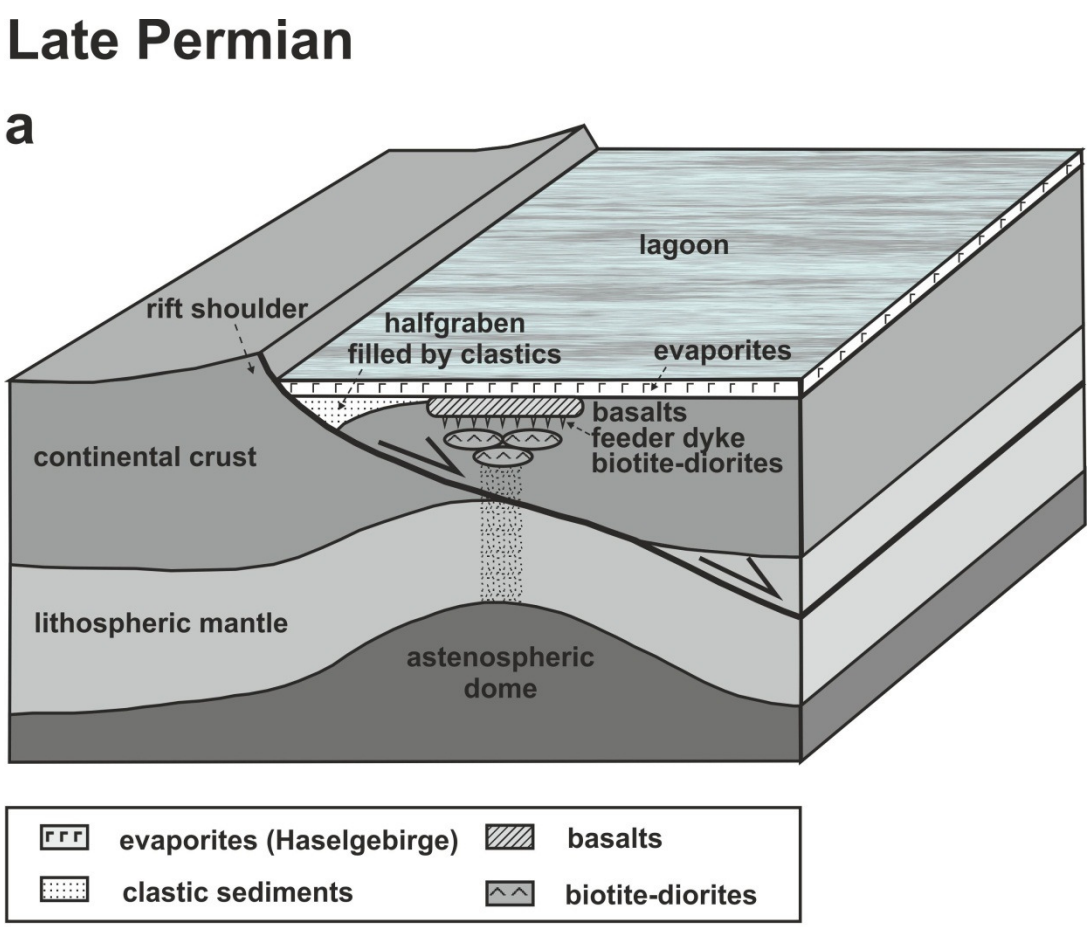

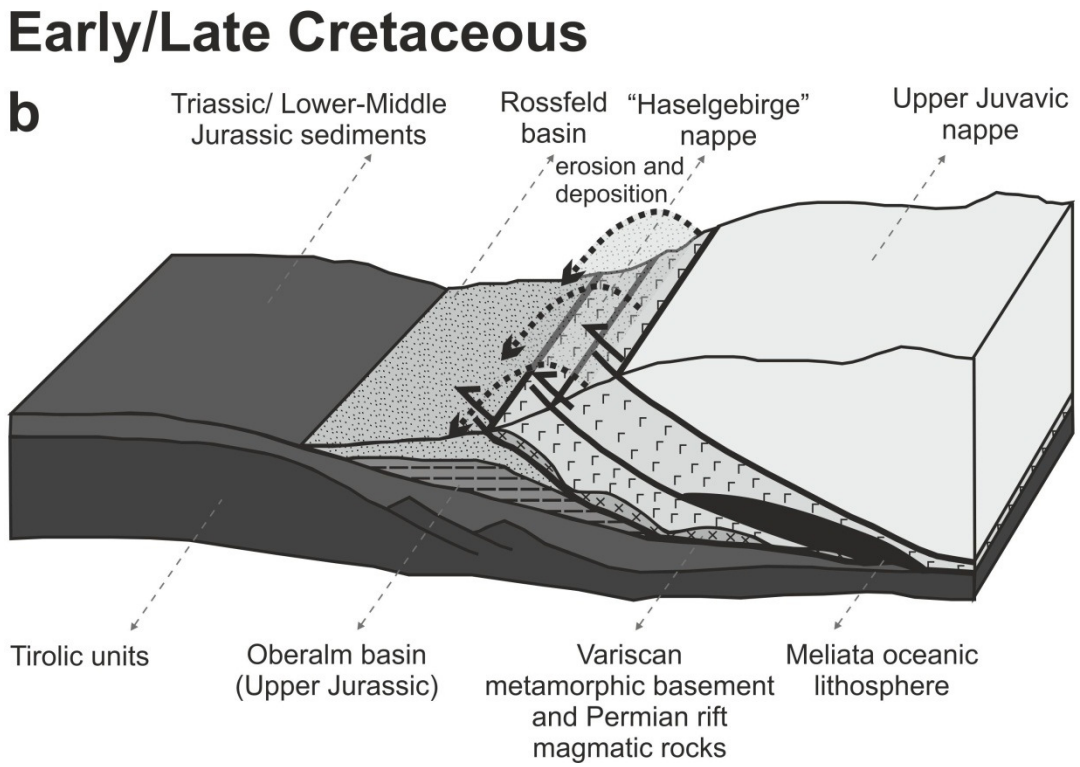

Fig. 12. Tectonic models for two steps of the tectonic evolution of the Austroalpine unit of Eastern Alps (after Schorn et al., Tectonophysics, revision submitted). a - Model of an asymmetric rift setting during Late Permian. b - Model of the tectonic emplacement of the Haselgebirge nappe over the Rossfeld Fms. of the Tirolic nappe complex.

8. Excursion stops

In the following the excursion points are shortly described (for their location see Fig. 3).

Stop 1: Anhydrite-carbonate mylonites

In the south-eastern part of level I (Fig. 6a) ductile structures related to thrusting of the Haselgebirge Fm. over the Lower to lowermost Upper Cretaceous is preserved close to the structural base of the Moosegg klippe in folded, nearly vertically dipping anhydrite and carbonate mylonites (Fig. 6b, d). The carbonate mylonite comprises millimeter-sized pyrite grains with pressure fringes indicating a well-expressed stretching lineation. The banded mylonites are nearly subvertically or steeply N-dipping, folded (Fig. 6c and d) and shear criteria indicate a top-west movement of the Haselgebirge nappe (Fig. 7a-d).
The banded carbonate mylonite (Fig. 6a) is about 10 meter thick, strongly foliated and shows a centimetre-scale, here subvertical, banding respectively foliation. The uppermost 50 cm of the carbonate mylonite are rich in pyrite, and show evidence for an axial plane foliation. Note, that banded mylonites are folded with subhorizontal fold axes, here described as fold axes F_2, and a cogenetic fracture cleavage (Fig. 6e), here tentatively assigned to S_2.
The banded anhydrite-carbonate mylonite (Fig. 6b and d) is exposed with a thickness of about four meters. It consists to ca. 75% of 0.5 – 4 cm thick anhydrite layers, which are separated by 3 - 4 cm thick layers of dark claystone (Fig. 6b). In addition to the pyrite lineation (Fig. 6c), we found evidence for an intersecting δ-lineation and evidence for an axial plane foliation.
The anhydrite-carbonate mylonite is 5 – 6 m thick and contains, in the lower part of the outcrop, a lot of pyrite, which shows a distinct stretching lineation (Fig. 6c). Furthermore, the banded mylonite rock comprises ca. 1 – 3 cm wide extension veins filled with in part fibrous gypsum (Fig. 6f). These are arranged in two orientations. The main orientation is subvertical, and fibres are oriented subperpendicular to vein walls. The subordinate veins are stepply E-dipping, and fibres have a similar orientation as in the main set. The similar orientation of fibres in both sets proves a cogenetic origin of both sets of gypsum-filled extensional veins.
The strongly foliated fine-grained anhydrite and carbonate mylonite is preserved with a WNW-trending, subhorizontal stretching lineation constituting together an L-S fabric indicating emplacement of the Haselgebirge evaporite mélange within ductile conditions (T > 240°C) taking the peak temperature estimates of Spötl et al. (Spötl et al., 1998, see Table 1). Furthermore, the steeply dipping axial plane foliation indicates E-W-folding.

Stop 2: In the south-eastern part of level I a ca. three meter thick, a strongly alterated greenstone lens mainly composed of meta-dolerites, meta-syenites and ultramafitites is exposed.

Stop 3: Brown, banded dolomite shows a dark brown lamination and is located in the western part of the levels II and III (Fig. 5h). This rock type has never been described before as a part of the Haselgebirge nappe and is quite rich in extension joints and blue Na-amphibole (riebeckite according to microprobe data).

Stop 4: Dark anhydrite with fibrous blue amphibole is located in the western part of level III (Fig. 5i). The numerous filaments of fibrous blue Na-amphibole (riebeckite) fill extension veins within the anhydrite. Their origin is likely due to rock/hydrothermal brine interaction, which is probably associated with ocean floor metamorphism.

Stop 5: As mentioned above the light gypsum, which is outcropped on level III, occurs in a syncline in the centre of Moosegg quarry (Fig. 5a). It is commonly massive and only in the upper rim partially foliated. Furthermore, some lenses of darker and internally strongly foliated lenses of coarse-grained anhydrite are interbedded (Fig. 5a).

Stop 6: Outcrops of biotite-diorite within dark gypsum breccia with two types of dark components are exposed on levels III and IV. The strongly foliated gypsum breccia contains two types of dark components (Fig. 5d). The first lenses are composed of cataclastically deformed, broken dark dolomite, which are rich in veins of white gypsum and very sulphurous in the centre of the lenses. The second type consists of dark, banded siliceous mudstone. Furthermore, some well preserved biotite-diorite blocks are embedded within the breccia.

Stop 7: The thin-bedded, brownish mica-rich greywacke is intercalated by shale and is located on the western rim of level III and can also be interpreted as an abyssal deposition. Thin-bedded brownish micritic limestones occur in a thick lens, but their assignment to the Werfen Fm. is not assured.

Stop 8: Red and green claystone comprise the bulk of a non-mined hill in the north-western part of level VI (Fig. 5e). These rocks were originally considered as siltstones of the Lower Triassic Werfen Fm.. However, the lamination and missing detrital white mica as well as the siliceous contents disprove this correlation.

Stop 9: The ductile Haselgebirge thrust fault is also exposed in the eastern part of level VIII (Fig. 4) within strongly weathered, dark and red gypsum mylonite. The gypsum crystals are ca. millimetre-sized, and we tentatively assume that the gypsum crystals were formed by secondary transformation from anhydrite.

Acknowledgements: We gratefully acknowledge (U-Th-Sm)/He apatite dating by István Dunkl (University of Göttingen) and Guoqing Han (Salzburg). We got support for the pilot study by the Stiftungs- und Förderungsgesellschaft of the University of Salzburg. The work has been completed within the project Polyhalite (grant no. P22,728) funded by the Austrian Science Fund (FWF).

References

Cox, K.J., Bell, J.D. and Pankhurst, R.J., 1979. The interpretation of igneous rocks. Allen and Unwin, London, 450 pp.

von Eynatten, H., Gaupp, R. and Wijbrans, J. R., 1996. $^{40}Ar/^{39}Ar$ laser-probe dating of detrital white micas from Cretaceous sedimentary rocks of the Eastern Alps: Evidence for Variscan high-pressure metamorphism and implications for Alpine orogeny. Geology, 24, 691–694.

Faupl, P. and Tollmann, A., 1978. Die Roßfeldschichten: Ein Beispiel für Sedimentation im Bereich einer tektonisch aktiven Tiefseerinne aus der kalkalpinen Unterkreide. Geologische Rundschau, 68, 93-120.

Frisch, W., Kuhlemann, J., Dunkl, I. and Székely, B., 2001. The Dachstein paleosurface and the Augenstein Formation in the Northern Calcareous Alps - a mosaic stone in the geomorphological evolution of the Eastern Alps. International Journal of Earth Sciences, 90, 500–518.

Gawlick, H.-J., Krystyn, L. and Lein, R., 1994. Conodont colour alteration indices: Palaeotemperatures and metamorphism in the Northern Calcareous Alps – a general view. Geologische Rundschau, 83, 660–664.

Götzinger, M.A. and Grum, W., 1992. Die Pb-Zn-F-Mineralisationen in der Umgebung von Evaporiten der Nördlichen Kalkalpen, Österreich – Herkunft und Zusammensetzung der fluiden Phase. Mitteilungen der Gesellschaft der Geologie- und Bergbaustudenten in Österreich, 38, 47–56.

Leitner, C., Neubauer, F., Urai. J. L. and Schoenherr, J., 2011. Structure and Evolution of a Rocksalt-Mudrock-Tectonite: the Haselgebirge in the Northern Calcareous Alps. Journal of Structural Geology, 33, 970–984. doi:10.1016/j.jsg.2011.02.008.

McDonough, W.F. and Sun, S.S. 1995. The composition of the Earth. Chemical Geology, 120, 223-254.

Pearce, J.A., 1982. Trace element characteristics of lavas from destructive plate boundaries. In: Thorpe, R.S. (ed.), Andesites: orogenetic Andesites and Related Rocks. Chichester, Wiley, pp. 525-548.

Pak, E. 1978. Schwefelisotopenuntersuchungen am Institut für Radiumforschung und Kernphysik II. Anzeiger der Österreichischen Akademie der Wissenschaften, Mathematisch-Naturwissenschaftliche Klasse, 115/1, 6-22.

Petrascheck, W.E., 1947. Der Gipsstock von Grubach bei Kuchl. Verhandlungen der Geologischen Bundesanstalt (1949), 148-152.

Rantitsch G., Russegger, B., 2005. Organic maturation within the Central Northern Calcareous Alps (Eastern Alps). Austrian Journal of Earth Sciences, 98, 68–76.

Schorn, A., 2010. The sulphatic Haselgebirge evaporite mélange revisited: evidence from the Moosegg quarry within central Northern Calcareous Alps. Master thesis Faculty of Natural Sciences, University of Salzburg, 139 pp.

Schorn, A. and Neubauer, F., 2011. Emplacement of an evaporitic melange nappe in central Northern Calcareous Alps: evidence from the Moosegg klippe (Austria). Journal of Austrian Earth Sciences, 104/2, 22–46.

Schorn, A., Neubauer, F. and Bernroider, M., 2012. The Haselgebirge evaporitic mélange in central Northern Calcareous Alps (Austria): part of the Permian to Lower Triassic rift of the Meliata ocean? Tectonophysics, revised version submitted.

Spötl, C., Kralik, M. and Kunk, M.J., 1996. Authigenic Feldspar as an Indicator of Paleo-Rock/Water Intercalations in Permian Carbonates of the Northern Calcareous Alps, Austria. J. Sed. Res., 66, 139–146.

Spötl, C., Longstaffe, F.J., Ramseyer, K., Kunk, M.J., Wiesheu, R., 1998. Fluid-rock reactions in an evaporitic mélange, Permian Haselgebirge, Austrian Alps. Sedimentology 45, 1019–1044.

Streckeisen, A. and Le Maitre, R.W., 1979. A chemical approximation to the modal QAPF classification of igneous rocks. Neues Jahrbuch Mineralogie Abhandlungen, 136, 169-206.

Sun, S.S. and McDonough, W.F., 1989 Chemical and isotopic systematics of ocean basalts: implications for mantle composition and processes. In: Saunders A.D. and Norry M.J. (eds.), Magmatism in ocean basin. Geological Society London Special Publication, 42, pp. 313-345.

Tollmann, A., 1985. Geologie von Österreich, Band 2. Wien, Deuticke, pp. 1–710.

Vozárová, A., Vozár, J. and Mayr, M., 1999. High-pressure metamorphism of basalts in the evaporitic sequence of the Haselgebirge: An evidence from Bad Ischl (Austria). Abhandlungen der Geologischen Bundesanstalt, 56, 325–330.

Wiesheu, R. 1997. Geologisch-geochemische Untersuchungen zur Rekonstruktion der thermischen Geschichte des Haselgebirges. Dissertation at the Technical University Munich, pp. 95.